Tone-Based Localization for Distinguishing Relative Locations in Wireless Sensor Networks

Chih-Yung Chang, *Associate Member, IEEE*, Chih-Yu Lin, and Chao-Tsun Chang

***Abstract*—Bounding-box mechanism is a well-known low-cost localization approach for wireless sensor networks. However, the bounding-box location information cannot distinguish the relative locations of neighboring sensors, hence leading to a poor performance for some applications such as location-aware routing. This paper proposes a *Differentiating Relative Locations* (*DRL*) mechanism which uses a mobile anchor to broadcast tones and beacons aiming at distinguishing the relative locations of any two neighboring nodes. With the order of entering and leaving tone transmission range, each sensor is able to identify its relative location relation with each of its neighbors. In addition, two path planning mechanisms are proposed to guarantee that all sensors can identify their relative locations while the energy consumption of the mobile anchor can be effective. Theoretical analysis is developed to estimate the impacts of duty time of tone signals in terms of energy conservation and accuracy of relative locations. Experimental study reveals that the proposed DRL mechanism effectively distinguishes relative locations of any two neighboring nodes and hence significantly improves the performance of location-aware routing in wireless sensor networks (WSNs).**

***Index Terms*—Localization, location-aware routing, relative locations, wireless sensor networks.**

I. Introduction

LOCALIZATION with low cost and high accuracy is of utmost importance for most applications in wireless sensor networks (WSNs). To eliminate the hardware cost on each static sensor or even remove the requirement of deploying a number of static anchors in the WSN, a number of bounding-box mechanisms [1]–[4] have been proposed based on a mobile anchor's assistance. Studies [1]–[4] assume that the mobile anchor can always be aware of its own location and periodically move and broadcast a beacon containing its up-to-date location for improving the location accuracy of the nearby sensors. Upon receiving the beacon message, the sensor nodes learn the fact that they are within the bounding-box region. Let $[a, b]$ denote a bounding-box where a and b are the coordinates of left-top and right-down points of the box. Let the transmission range of mobile anchor be r and the beacon coordinate received by sensor s be (x, y). By applying the bounding-box mechanisms, the sensor s learns that its location is within the bounding-box region $[(x - r, y + r), (x + r, y - r)]$.

Manuscript received May 19, 2011; revised June 25, 2011; accepted July 24, 2011. Date of publication August 04, 2011; date of current version April 11, 2012. The associate editor coordinating the review of this paper and approving it for publication was Prof. Ralph Etienne-Cummings.

C.-Y. Chang and C.-Y. Lin are with the Department of Computer Science and Information Engineering, Tamkang University, Tamsui 25137, Taipei, Taiwan (e-mail: cychang@mail.tku.edu.tw; cylin@wireless.cs.tku.edu.tw).

C.-T. Chang is with the Department of Information Management, Hsiuping University of Science and Technology, Dali 41280, Taichung, Taiwan (e-mail: cctas@mail.hust.edu.tw).

Color versions of one or more of the figures in this paper are available online at http://ieeexplore.ieee.org.

Digital Object Identifier 10.1109/JSEN.2011.2163503

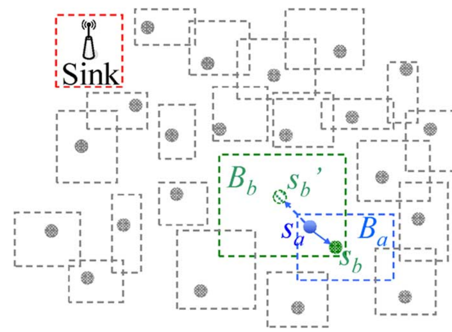

Fig. 1. Distinguishing relative locations of neighboring sensors has a significant impact on location-aware routing performance.

Though existing bounding-box approaches provide each sensor with bounding-box location information, however, they cannot distinguish relative locations of the neighboring sensors. When sensors perform some location-aware applications such as routing schemes [5]–[8], a poor performance will be obtained. Fig. 1 gives an example for illustrating that distinguishing relative locations for neighboring sensors has a significant impact on location-aware routing performance. Let B_i denote the bounding-box of sensor s_i. As shown in Fig. 1, sensor s_a receives a packet and intends to apply the location-aware routing which forwards the packet to the neighbor closest to the sink. In this example, sensor s_a will forward the packet to s_b because B_b is likely closer to the sink than B_a. However, the physical location of s_b is located at the right-down direction of s_a. As a result, the packet is forwarded to an improper node, increasing the routing length.

This paper proposes a DRL mechanism which is extension of the existing bounding-box approaches. The proposed DRL mechanism not only provides each sensor with an estimated bounding-box location but also helps each pair of neighboring sensors distinguish their relative locations. The key idea of the proposed DRL mechanism is to employ a mobile anchor broadcasting tone signals to distinguish the relative locations. The proposed DRL mechanism mainly consists of two components: *distinguishing relative location strategy* and *path planning strategy*. First of all, a set of rules are developed for each sensor to distinguish its relative location with its neighbors based on the order of entering and leaving tone-signal range. Then, two efficient path planning strategies are proposed for the mobile anchor to visit the whole monitoring region with low power consumption while the relative locations of all sensors are distinguishable.

The remaining part of this paper is organized as follows. Section II illustrates the network environment and problem formulation of our approach. Sections III and VI present the details of DRL mechanism. Sections V and VI investigate the theoretical analysis and the performance of the proposed DRL mechanism, respectively. Finally, the conclusions are given in Section VII.

II. Network Environment and Problem Formulation

A. Network Environment

This paper assumes that n sensor nodes are randomly distributed in an area sized by $L \times W$. Let S denote the set of all sensor nodes in the monitoring region and let $H(s_i)$ denote the set of neighbors of sensor s_i. In addition, a mobile anchor that is aware of its location can broadcast three types of signals, including two types of tone and one type of beacon message. The beacon message contains the current location information of the mobile anchor and the tone signal consumes smaller energy than beacon message since it does not carry any information.

In WSNs, routing is a very important application. If each sensor only has relative location information but is not aware of its own physical location information, it cannot forward the sensing data to the destination node in an efficient way. This is because that the source node or the forwarding node does not know the direction at which the destination node is located. Consequently, the mobile anchor has to broadcast not only two types of tone but also one type of beacon message that contains its current physical location information. Then, by applying the existing bounding-box approaches [1]–[4] and our proposed DRL mechanism, the routing performance can be improved significantly.

B. Problem Formulation

This paper extends the bounding-box approach aiming at distinguishing the relative location of two neighboring sensors. One major task of this paper is to develop rules for each sensor to distinguish its relative location with its neighbors in a distributed manner. The other task is to establish an energy-efficient path for mobile anchor so that all sensors can be visited by the mobile anchor.

Snake-like path has been generally applied in network deployment and patrolling for WSNs. In this paper, the path construction for mobile anchor is discussed based on the snake-like path $P(w)$, as shown in Fig. 2, where the snake length and width are $L+2r$ and w, respectively. To evaluate the energy consumption of the mobile anchor, a set of notations are introduced. Let e_{move} and e_{turn} denote the energy consumptions required for mobile anchor moving for a unit distance and turning a corner, respectively. Furthermore, let e_{tone} denote the energy consumption required for mobile anchor broadcasting tone signal for a time unit and e_{beacon} denote the energy required for mobile anchor broadcasting a beacon message. Let a *broadcasting cycle* ρ be a fix time period that mobile anchor continuously broadcasts the tone signal and broadcasts one beacon message in the end of the cycle. Let $E(P,\rho)$ denote the total energy consumption for the mobile anchor that moves along the snake-like path $P(w)$ for a *broadcasting cycle* ρ. Furthermore, let r and v denote the transmission range and moving speed of a mobile anchor, respectively. In the snake-like path $P(w)$, each row has length $L+2r$ and a beacon is broadcasted every length of ρv. Therefore, there are $\lfloor L+2r/\rho v \rfloor$ beacons broadcasted in the movement of each row. The total energy consumption E_{beacon} for broadcasting beacon message can be measured by the following:

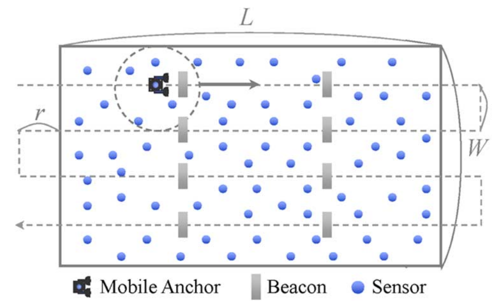

Fig. 2. The path construction for mobile anchor is discussed based on the snake-like path.

$$E_{beacon} = e_{beacon} \left[\lfloor (L+2r)/\rho v \rfloor \times \lfloor W/w \rfloor \right]. \quad (1)$$

Since the mobile anchor always broadcasts tone signals except broadcasting beacons, the movement length for broadcasting tone signal is the total length minus the length for broadcasting beacons. As a result, the total energy consumption for broadcasting tone signals is measured by

$$E_{tone} = e_{tone} \left[(L+2r) \times \lfloor W/w \rfloor - ((L+2r)/\rho v) \times \lfloor W/w \rfloor \right]. \quad (2)$$

The total energy consumption for the mobile anchor turning corners is calculated by counting the number of turns in path $P(w)$, as shown as follows:

$$E_{turn} = e_{turn} \times 2 \left(\lfloor W/w \rfloor - 1 \right). \quad (3)$$

In addition, the total energy consumption for movement is calculated based on the total path length of $P(w)$, as follows:

$$E_{move} = e_{move} \left[(L+2r) \times \lfloor W/w \rfloor + w \times \left(\lfloor W/w \rfloor - 1 \right) \right]. \quad (4)$$

Hence, the total energy consumption $E(P,\rho)$ is the total sum of energy consumptions for moving, making turns and broadcasting beacon and tone signals as follows:

$$E(P,\rho) = E_{move} + E_{turn} + E_{beacon} + E_{tone}. \quad (5)$$

In order to conserve the energy consumption for mobile anchor, Expression (6) depicts the constraint of maximum energy consumption

$$E(P,\rho) \le E_{\max}. \quad (6)$$

By receiving the beacons from the mobile anchor, each sensor node can learn its location information which is a rectangular region $[(s_i.x_1, s_i.y_1), (s_i.x_2, s_i.y_2)]$. This paper has two major goals. First, we aim to distinguish relative locations for neighboring sensors. Statement (7) depicts the goal of this paper that

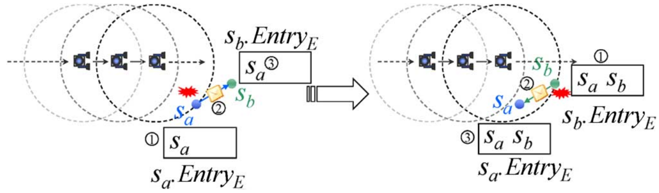

Fig. 3. Sensors s_a and s_b distinguish their relative locations with each other based on their $Entry_E$ tables.

any sensor s_i can distinguish with any neighboring sensor s_j the relative locations in x-coordinate and y-coordinate directions

$$\forall s_j \in H(s_i) \Rightarrow s_i.x\Delta s_j.x \text{ and } s_i.y\Delta s_j.y, \quad \text{where } \Delta \in \{>,=,<\}. \quad (7)$$

III. DRL Properties

This section initially introduces the basic concepts of the proposed DRL mechanism. Then, the details of DRL are presented.

A. Basic Concept

The basic concept of DRL is to distinguish the relative locations of each pair of neighboring sensors based on the order of entering and leaving the tone-single range. To achieve this, each sensor node should maintain an $Entry_E$ table in its own cache. The following gives an example to show the basic concept of DRL mechanism.

Assume that the mobile anchor moves in the right direction. We show the operations what each sensor should perform when it enters or leaves the tone-signal range. In Fig. 3, consider two neighboring sensors s_a and s_b. When sensor s_a enters tone-signal range, it records its sensor ID in its $Entry_E$ table and then broadcasts its ID $= s_a$ to all of its neighbors. Upon receiving the message from sensor s_a, sensor s_b records ID of s_a in its $Entry_E$ table. Afterward, when sensor s_b enters the tone-signal range, it similarly records its ID in the $Entry_E$ table and then broadcasts a message containing its own ID $= s_b$. When s_a receives this message, it records the ID of s_b in its $Entry_E$ table. According to the order of IDs recorded in $Entry_E$ tables, sensors s_a and s_b learn the fact that sensor s_a is located at the left side of sensor s_b.

Although using the order of entering tone-signal range can generally distinguish the relative locations of each pair of neighbors, however, the *Table Ambiguous* and *Location Ambiguous Problems* exist. Fig. 4 gives an example of the *Table Ambiguous Problem*. In Fig. 4, sensors s_a and s_b enter tone-signal range at the same time and hence they cannot distinguish their relative locations. Fig. 5 further depicts an example of the *Location Ambiguous Problem*. In Fig. 5, sensor s_a enters tone-signal range earlier than s_b but it is invalid if we conclude that sensor s_a is located at the left side of s_b. This implies that the relative location cannot be correctly determined in some cases.

B. Handling the Table Ambiguous Problem

To cope with the *Table Ambiguous Problem*, additional table $Exit_E$ should be constructed to record the order of sensors

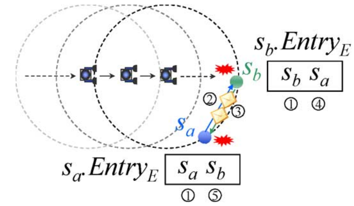

Fig. 4. Sensors s_a and s_b enter tone-signal at the same time and hence they cannot distinguish their relative locations.

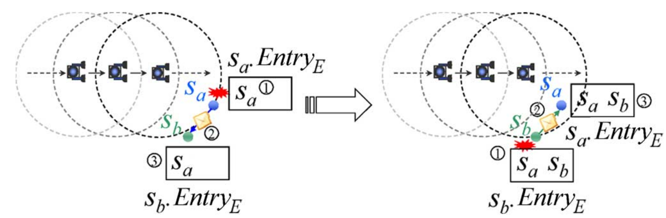

Fig. 5. Relative location cannot be correctly determined because that the shape of tone-signal range is a disc.

leaving tone-signal range. The operations for maintaining $Entry_E$ and $Exit_E$ tables are described below. Any sensor, say s, that enters (leaves) the tone-signal range should firstly record its ID in its $Entry_E(Exit_E)$ table and then broadcasts its ID. Upon receiving the broadcasting message, all neighboring sensors of s should record the ID of s in their own $Entry_E(Exit_E)$ tables.

Let notations T_s^{in} and T_s^{out} denote the time points that sensor s enters and leaves the tone-signal range, respectively. The following gives the definitions of entering and leaving orders of any pair of neighboring sensors.

Definition 1. The Entering Order $s_a\delta s_b$: Let $s_a\delta s_b$ denote the order of any pair of neighboring sensors s_a and s_b entering the tone-signal range, where $\delta \in \{<_{In}, >_{In}, =_{In}\}$. The values of δ are $<_{In}, >_{In}$, or $=_{In}$ if conditions $T_a^{in} < T_b^{in}$, $T_a^{in} > T_b^{in}$, or $T_a^{in} = T_b^{in}$ hold, respectively. □

For instance, if s_a enters tone-signal range earlier than s_b, we have $T_a^{in} < T_b^{in}$. It also implies the relation of $s_a <_{In} s_b$.

Definition 2. The Leaving Order $s_a\varepsilon s_b$: Let $s_a\varepsilon s_b$ denote the order of any pair of neighboring sensors s_a and s_b leaving the tone-signal range, where $\varepsilon \in \{<_{Out}, >_{Out}, =_{Out}\}$. The values of ε are $<_{Out}, >_{Out}$, or $=_{Out}$ if conditions $T_a^{Out} < T_b^{Out}$, $T_a^{Out} > T_b^{Out}$, or $T_a^{Out} = T_b^{Out}$ hold, respectively. □

For instance, when s_a leaves tone-signal range earlier than s_b, denoted by $T_a^{Out} < T_b^{Out}$, it implies that we have $s_a <_{Out} s_b$.

Furthermore, let $s_i \| s_j$ represents that sensor s_i is located at the left side of s_j. Next, we discuss some properties based on the records of $Entry_E$ and $Exit_E$ tables. Three lemmas are therefore developed to help each pair of sensors distinguish their relative locations in a distributed manner.

Lemma 1: The relation $s_a \| s_b$ holds if we have the facts $s_a <_{In} s_b$ and $s_a <_{Out} s_b$.

Proof: As shown in Fig. 6(a), when sensor s_a enters tone-signal range, sensor s_b must be located in the shadow region due to the fact $s_a >_{In} s_b$. Similarly, as shown in Fig. 6(b), when sensor s_a leaves tone-signal range, sensor s_b must also be located in the shadow region because of the fact $s_b <_{Out} s_a$.

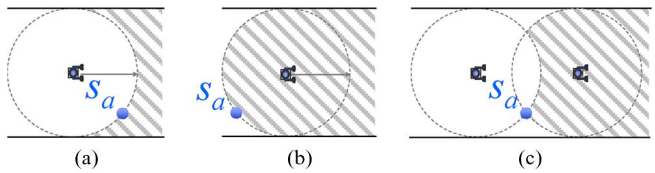

Fig. 6. The scenario applied in the proof of Lemma 1: (a) The moment that s_a enters tone-signal range. (b) The moment that s_a leaves tone-signal range. (c) The combination of Fig. 6(a) and (b).

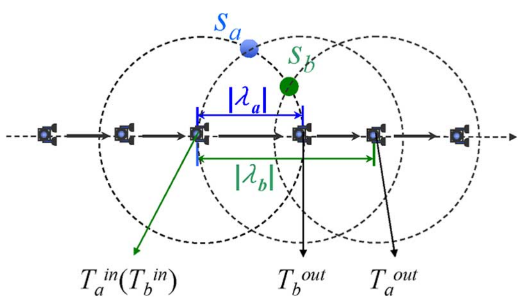

Fig. 7. If sensors s_a and s_b enter tone-signal range at the same time, they can distinguish their relative location relation by comparing the values of $|\lambda_a|$ and $|\lambda_b|$.

As shown in Fig. 6(c), we can conclude that sensor s_b must be located in the intersection area of the two shadow regions shown in Fig. 6(a) and (b). This implies that the relation $s_a||s_b$ holds.□

According to Lemma 1, each pair of sensors s_a and s_b can locally distinguish their relative locations by checking their own $Entry_E$ and $Exit_E$ tables. The following rule is accordingly proposed.

General Rule: If the orders of any pair of neighboring sensors s_a and s_b in $Entry_E$ and $Exit_E$ are $s_a <_{In} s_b$ and $s_a <_{Out} s_b$, respectively, the relation $s_a||s_b$ holds. □

Although the *General Rule* can generally distinguish the relative locations of a pair of neighbors, however, the *Table Ambiguous Problem* still exists. The following further presents Lemma 2 to overcome this problem.

Lemma 2: The relation $s_a||s_b$ holds if mobile anchor moves in a constant speed v and the conditions $s_a =_{In} s_b$ and $s_a <_{Out} s_b$ hold.

Proof: The fact $s_a =_{In} s_b$ implies that sensors s_a and s_b enter tone-signal range at the same time, as shown in Fig. 7(a). Let the *trajectory associated with sensor* s, denoted by λ_s, represent the mobile anchor's trajectory from T_s^{in} to T_s^{out}. Fig. 7 shows the trajectories associated with sensors s_a and s_b, respectively. Since the mobile anchor moves in a constant speed v, the lengths of λ_a and λ_b can be calculated as follows:

$$|\lambda_a| = \left(T_a^{out} - T_a^{in}\right) \times v \text{ and } |\lambda_b| = \left(T_b^{out} - T_b^{in}\right) \times v. \quad (8)$$

From the fact $s_a =_{In} s_b$, we have the relation of $T_a^{in} = T_b^{in}$. In addition, the fact $s_a <_{Out} s_b$ implies that the relation $T_a^{Out} < T_b^{Out}$ holds. Substitute the two relations into (8), we have the property $|\lambda_a| < |\lambda_b|$, which implies that the relation $s_a||s_b$ holds. □

The proposed Lemma 2 is useful to cope with the *Table Ambiguous Problem* when the two sensors cannot distinguish their relative location because of their timestamps of entering tone single are identical. The following further presents another lemma to tackle the problem that their timestamps of leaving tone single are identical.

Lemma 3: The relation $s_a||s_b$ holds if mobile anchor moves in a constant speed v and we have the facts $s_a =_{Out} s_b$ and $s_a <_{In} s_b$.

Proof: We omit the proof of Lemma 3 since it is similar to that of Lemma 2. □

The Lemmas 2 and 3 help each pair of sensors cope with the *Table Ambiguous Problem*. Sensor s_a selects any of its neighbors, say s_b, and locally checks its $Entry_E$ and $Exit_E$ tables. If their orders in $Entry_E$ or $Exit_E$ tables are different, it represents that s_a and s_b enter or leave tone-signal range at the same time. Sensors s_a and s_b can distinguish their relative locations based on the following two rules.

Enter-Table Ambiguous (ETA) Rule: The relation $s_a||s_b$ holds if the following two criteria are satisfied.

1) The relation $s_a =_{In} s_b$ holds.
2) The orders of sensors s_a and s_b in their $Exit_E$ tables are $s_a <_{Out} s_b$.

□

Exit-Table Ambiguous (XTA) Rule: The relation $s_a||s_b$ holds if the following two criteria are satisfied.

1) The relation $s_a =_{Out} s_b$ holds.
2) The orders of sensors s_a and s_b in their $Entry_E$ tables are $s_a <_{In} s_b$.

□

Herein, we notice that it might cause a collision problem if sensors s_a and s_b enter or leave tone-signal range at the same time and hence they broadcast *Entering* or *Leaving messages* simultaneously. To cope with this problem, we additionally introduce *collision-free time-stamp mechanism*. When a sensor enters or leaves tone-signal range, it waits for a random time t and then broadcasts *Entering* or *Leaving messages* which contain the value of t. As a result, the collision problem can be avoided while they can maintain the valid $Entry_E$ and $Exit_E$ tables.

This subsection initially proposes the *General Rule* for each sensor to distinguish its relative location from each neighbor. The *ETA* and *XTA* rules are also proposed to cope with the *Table Ambiguous Problem*. The next subsection will present another rule for handling the *Location Ambiguous Problem* which is more complicated than the *Table Ambiguous Problem*.

C. Handling the Location Ambiguous Problem

This subsection aims to cope with the *Location Ambiguous Problem*. For simplicity and without loss of generality, we discuss the *Location Ambiguous Problem* by considering the scenarios that s_a enters tone-signal range earlier than s_b, but s_b leaves tone-signal range earlier than s_a, as shown in scenarios shown in Fig. 8(a) and (b).

Although the $Entry_E$ and $Exit_E$ tables in Fig. 8(a) are identical to those in Fig. 8(b), the relative locations of s_a and s_b in Fig. 8(a) and (b) are totally different. That is, the relation $s_a||s_b$ holds in Fig. 8(a) while the relation $s_b||s_a$ holds in Fig. 8(b). As a result, relative location cannot be correctly determined because the shape of tone-signal range is a disc and the two sensors are too close with each other. For the ease of presentation, scenarios shown in Fig. 8(a) and (b) are referred to *a_Left* and

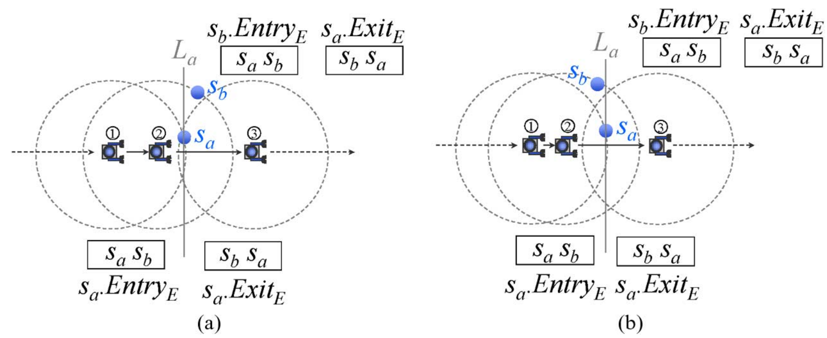

Fig. 8. Two scenarios that have the same contents in $Entry_E$ and $Exit_E$ tables but have different relative location relations. (a) The first scenario arisen the *Location Ambiguous Problem*. (b) The second scenario arisen the *Location Ambiguous Problem*.

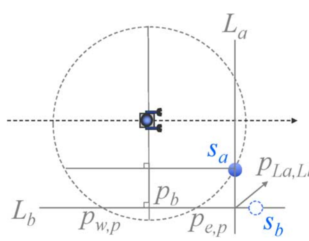

Fig. 9. If $d > 0$, the relation $s_a \| s_b$ holds. Otherwise, the relation $s_b \| s_a$ holds.

a_Right scenarios, respectively. We observe that the only difference of the two scenarios depicted in Fig. 8(a) and (b) is that s_b is located at the different sides of line L_a. To tackle the location ambiguous problem, the following introduces some notations for illustrating how we can identify that the current situation belongs to *a_Left* or *a_Right* scenarios.

Let $dis(i, j)$ denote the distance between locations i and j, and $loc(s_i)$ denote the location of sensor s_i. Consider Fig. 9 where the circle denotes the tone signal range of the mobile anchor. Let L_a denote the line passing through $loc(s_a)$ but parallelizing to y-axis. Let L_b denote the line passing through $loc(s_b)$, but perpendicular to L_a. Let p_b denote the midpoint of $p_{w,p}$ and $p_{e,p}$, where $p_{w,p}$ and $p_{e,p}$ denote the left and right intersection points of L_b and transmission circle of the mobile anchor, respectively. Let $P_{La,Lb}$ denote the intersection point of L_a and L_b. The following defines *Decision Value* d which will be used to identify the current situation belonging to *a_Left* or *a_Right* scenarios.

Definition 3. Decision Value d: Assume that there are two neighboring sensors s_a and s_b, and the relation $s_a <_{In} s_b$ holds. The *Decision Value* d is the difference value of $dis(loc(s_b), p_{e,p})$ and $dis(P_{La,Lb}, p_{e,p})$. That is,

$$d = dis\,(loc(s_b), p_{e,p}) - dis(p_{La,Lb}, p_{e,p})$$

□

The following Lemma aims to cope with the *Location Ambiguous Problem*.

Lemma 4: Assume that the ambiguous relations $s_a <_{In} s_b$ and $s_a >_{Out} s_b$ hold. The relation $s_a \| s_b$ holds if $d > 0$. Otherwise, the relation $s_b \| s_a$ holds.

Proof: In case of $d > 0$, the value of $dis(loc(s_b), p_{e,p})$ is larger than the value of $dis(P_{La,Lb}, P_{e,p})$. It implies that s_b is located at the right side of the L_a. This implies that the relation $s_a \| s_b$ holds. Similarly, it can be proved that the relation of $s_b \| s_a$ holds in case of $d < 0$. □

Lemma 4 helps each sensor deals with the *Location Ambiguous Problem*. Sensor s_a selects any of its neighbor s_b and locally checks its $Entry_E$ and $Exit_E$ tables. If the $Entry_E$ and $Exit_E$ tables of s_a are totally identical to those of s_b, but the orders of s_a and s_b in the two $Entry_E$ tables collide with those in the two $Exit_E$ tables, the *Location Ambiguous Problem* occurs. Sensor s_a can distinguish its relative location with any neighbor s_b by applying the following rule.

Location Ambiguous (LA) Rule: The relation $s_a \| s_b$ holds if the following three criteria are satisfied.

1) The orders of sensors s_a and s_b in their $Entry_E$ tables are $s_a <_{In} s_b$;
2) The orders of sensors s_a and s_b in their $Exit_E$ tables are $s_b <_{Out} s_a$;
3) $d > 0$.

□

The following gives a theorem to prove that each pair of neighboring sensors can distinguish their relative locations with each other based on the proposed four rules: *General*, *ETA*, *XTA* and *LA Rules*.

Theorem 1: Each sensor can apply the proposed General, ETA, XTA and LA Rules to distinguish the relative locations with each of its neighbors.

Proof: Let sensors s_a and s_b be any pair of neighboring sensors. When the mobile anchor moves along the right direction and broadcasts tone signal, the orders of s_a and s_b for entering or leaving tone-signal range can be divided into nine cases. In Table I, each sensor checks its $Entry_E$ and $Exit_E$ tables to identify the case it belongs and then applies the corresponding rule as given in the *Applied_Rule* column of Table I. As a result, it can distinguish the relative locations with each of its neighbors, as shown in the *Result* column in Table I. In particular, when the situation of case 9 occurs, sensors s_a and s_b enter and then leave tone-signal range at the same time, respectively. That is, they fall on the line that is perpendicular to the x-axis. This indicates that they have the same x-coordinate. Hence, the *Applied_Rule* and the *Result* are “No Need” and “Not Important,” respectively. □

IV. Moving Path for Mobile Anchor

In the previous section, four rules are proposed to distinguish relative location of each pair of neighboring sensors. How-

TABLE I
APPLIED RULE AND RESULT OF RELATIVE LOCATION CORRESPONDING TO EACH CASE

Case	Relation	Applied_Rule	Result
1	$s_a <_{In} s_b$ and $s_a <_{Out} s_b$	General Rule	$s_a \parallel s_b$
2	$s_a >_{In} s_b$ and $s_a >_{Out} s_b$		$s_b \parallel s_a$
3	$s_a =_{In} s_b$ and $s_a <_{Out} s_b$	ETA Rule	$s_a \parallel s_b$
4	$s_a =_{In} s_b$ and $s_a >_{Out} s_b$		$s_b \parallel s_a$
5	$s_a <_{In} s_b$ and $s_a =_{Out} s_b$	XTA Rule	$s_a \parallel s_b$
6	$s_a >_{In} s_b$ and $s_a =_{Out} s_b$		$s_b \parallel s_a$
7	$s_a <_{In} s_b$ and $s_a >_{Out} s_b$	LA Rule	$d > 0 \Rightarrow s_a \parallel s_b$
			$d < 0 \Rightarrow s_b \parallel s_a$
8	$s_a >_{In} s_b$ and $s_a <_{Out} s_b$		$d > 0 \Rightarrow s_b \parallel s_a$
			$d < 0 \Rightarrow s_a \parallel s_b$
9	$s_a =_{In} s_b$ and $s_a =_{Out} s_b$	No Need	Not Important

ever, the four rules should be operated under the criteria that all sensor can receive tone signals from mobile anchor. Based on the snake-like trajectory, this section proposes two path planning mechanisms to guarantee that all sensors can receive tone signals while the energy consumption of the mobile anchor can be reduced. The path planning mechanism will be implemented on the mobile anchor. Initially, we propose a *Two-Phase DRL* mechanism which simply asks mobile anchor moving along the horizontal direction in the first phase and then moves along the vertical direction in the second phase. To save the energy consumption of mobile anchor, we propose the *Single-Phase DRL* mechanism, which asks mobile anchor only moving along the horizontal direction, while all sensors are guaranteed to receive the tone signals as well.

A. Two-Phase DRL Mechanism With Tones

The *Two-Phase* snake-like path is shown in Fig. 2 where the snake length is $L+2r$ and the snake width is r. In the first phase, as shown in Fig. 2, the mobile anchor moves along the right direction and then moves along the left direction in turn. Since the snake width is r, each sensor can receive the tone signals and use *General*, *ETA*, *XTA* and *LA Rules* to distinguish the relative locations with each of its neighbors in terms of the horizontal direction. Similarly, the mobile anchor will move along the vertical direction in the second phase. As a result, each sensor can also apply the proposed four rules to distinguish the relative locations with each of its neighbors in terms of the vertical direction.

Herein, we notice that the four rules proposed in the previous section are developed based on the assumption that the mobile anchor moves along the right direction. When the mobile anchor moves along the left direction, the results by applying four rules should be opposite. Hence, each sensor should be aware the movement direction of the mobile anchor before it applies the four rules. Two types of tone signal, namely TS_e and TS_w, are broadcasted by mobile anchor to indicate that its movement is along the right or the left directions, respectively. Similarly, in the second phase, the mobile anchor uses two types of tone-signal, namely TS_n and TS_s, to indicate that its movement is along the north or the south directions, respectively.

B. Single-Phase DRL Mechanism With Tones

This subsection further proposes *Single-Phase DRL* mechanism aiming at improving the energy consumption of the *Two-Phase DRL* mechanism. In the *Single-Phase DRL* mechanism, mobile anchor moves along the horizontal direction only, as shown in Fig. 2. The distance between two horizontal trajectories is r which is identical to the communication range of the mobile anchor. This can guarantee that all sensors can receive tone signals from the mobile anchor and then determine the relative locations. Compared with the *Two-Phase DRL* mechanism, the *Single-Phase DRL* mechanism saves the movements along the vertical direction. The most challenge of designing the *Single-Phase DRL* mechanism is that it is difficult for each sensor to determine its relative location in terms of the vertical direction. The following gives an example to illustrate how the *Single-Phase DRL* mechanism overcomes this challenge.

Recall that the *trajectory associated with sensor* s, denoted by λ_s, represents the mobile anchor's trajectory from T_s^{in} to T_s^{out}. Consider Fig. 7. When sensors s_a and s_b enter the tone-signal range, they can calculate $|\lambda_a|$ and $|\lambda_b|$ according to (8), respectively. Obviously, if a sensor has longer duration time for receiving tone signal than the other, it must be closer to the mobile anchor's movement trajectory. That is to say, the sensor which has larger value of λ is closer to the anchor's trajectory. From this observation, the fact of $|\lambda_b| > |\lambda_a|$, as shown in Fig. 7, implies that s_b is closer to the mobile anchor's movement trajectory than s_a. Since they are both located above the anchor's movement trajectory, and s_b is closer to the anchor's movement trajectory, we imply that sensor s_b is located below the sensor s_a.

To generalize the discussion of the above example, the following considers two cases, depending on whether or not sensors s_a and s_b are located at the same side of the trajectory.

Case 1. Same Side of Trajectory: This case considers that neighboring sensors s_a and s_b are located at the same side of the trajectory. This implies that s_a and s_b are both located above or below the anchor's movement trajectory.

Let notation $s_i//s_j$ represent that sensor s_i is located above s_j. There are two different results if we have $|\lambda_a| > |\lambda_b|$. One is that both sensors s_a and s_b are located above the anchor's movement trajectory. The fact $|\lambda_a| > |\lambda_b|$ implies that s_a is closer to the anchor's trajectory than s_b. Therefore, the relation $s_b//s_a$ holds. The other is that if sensors are both located below the anchor's movement trajectory and $|\lambda_a| > |\lambda_b|$, the relation $s_a//s_b$ holds. The following λ-Property reflects this observation.

λ-Property: The relation $s_a//s_b(s_b//s_a)$ holds if sensors s_a and s_b satisfy the following criteria.

1) Both sensors s_a and s_b are located below (above) the anchor's trajectory.
2) $|\lambda_a| > |\lambda_b|$ holds.

□

According to the λ-Property, sensors s_a and s_b can distinguish their relative locations in terms of vertical direction. However, the λ-Property can work only if sensors s_a and s_b can know that they are located at the same side of the anchor's movement trajectory. The following further discusses how sensors s_a and s_b are able to know whether or not they are located at the same side of the trajectory.

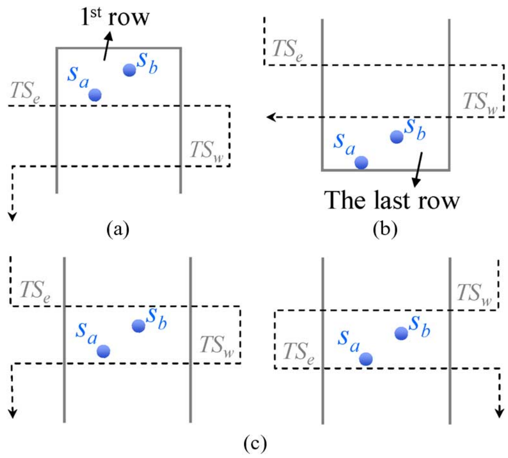

Fig. 10. There are three possible situations that sensors s_a and s_b can know whether or not they are located at the same side of the anchor's trajectory.

Recall that TS_e and TS_w denote the tone signal broadcasted when the mobile anchor moves along right and left directions, respectively. Consider that sensors s_a and s_b to be a neighboring pair and they intend to know whether or not they are located at the same side of the anchor's movement trajectory. Let the trajectories of snake-like movement of the mobile anchor partitions the whole monitoring region into several rows. There are three possible situations as shown in Fig. 10(a)–(c). Fig. 10(a) and (b) depict that both sensors s_a and s_b are located at the first row and last row of the monitoring region and thus they receive only single tone signal TS_e and TS_w, respectively, while Fig. 10(c) depicts that they are located neither first row nor last row and thus both of them must receive two tone signals TS_e and TS_w. The following details how sensors s_a and s_b can be aware that whether or not they are located at the same side of the trajectory in each situation.

Situation 1. Consider Fig. 10(a). Sensors s_a and s_b only receive TS_e. Obviously, this implies that both of them are located at the first row and thus they are located at the same side of the trajectory. □

Situation 2. The discussion of this situation is similar to that of Situation 1. Consider Fig. 10(b). Both sensors s_a and s_b are located at the last row and thus they are located at the same side of the trajectory. □

Situation 3. Consider Fig. 10(c). In this situation, both sensors s_a and s_b receives two tone signals TS_e and TS_w. Let $s_i.TS_x$ denote the time for sensor s_i receiving TS_x, where $x \in \{e, w\}$. It is obvious that sensors s_a and s_b are located at the same side of the trajectory if either of the criteria (C1) and (C2) holds

$$s_a.TS_e < s_a.TS_w \text{ and } s_b.TS_e < s_b.TS_w \quad \text{(C1)}$$
$$s_a.TS_w < s_a.TS_e \text{ and } s_b.TS_w < s_b.TS_e \quad \text{(C2)}$$

□

Based on the above discussions, we guarantee that sensors s_a and s_b can be aware that whether or not they are located at the same side of the trajectory. If it is the case, they are able to apply the λ-Property for distinguishing their relative location. Otherwise, they are located at different side of the trajectory, which will be discussed in the next case.

Case 2. Different Side of Trajectory: This case considers that neighboring sensors s_a and s_b which are located at the different side of the trajectory. The following discusses three possible situations.

Situation 1. The fact that sensor s_a only receives TS_e implies that sensor s_a is located at the first row. Consequently, we have the fact that $s_a//s_b$ holds. □

Situation 2. The fact that sensor s_a only receives TS_w implies that sensor s_a is located at the last row. Consequently, we have the fact that $s_b//s_a$ holds. □

Situation 3. In this situation, sensor s_a receives two tone signals TS_e and TS_w. There are two conditions. One is that s_a receives TS_e earlier than TS_w and another is that s_a receives TS_w earlier than TS_e. Since the discussions of two conditions are similar, without the loss of generality, we only discuss the first condition that the times for s_a and s_b receiving tone signal TS_e differ a little but the times for them receiving the tone signal TS_w differ a lot. Sensors s_a and s_b can utilize the tone signal TS_w, which creates a large difference in receiving times of sensors s_a and s_b, to distinguish their relative location. That is, sensors s_a and s_b can be aware the fact of $s_b//s_a$ since the fact $s_b.TS_w < s_a.TS_w$ holds. □

V. Theoretical Analysis

The proposed DRL mechanism can help each pair of neighboring sensors distinguish their relative locations. However, DRL mechanism results in significant energy cost if the mobile anchor always broadcasts tone signals during the process. One approach for saving the energy consumption of DRL is that mobile anchor keeps silence for a while during its movement. That is, the duty time of broadcasting tone signal is ξ in every time period T. However, this way might introduce some location inaccuracy, where some neighboring sensors might not distinguish their relative locations. This section presents the theoretical analysis for the tradeoff between energy conservation and location accuracy. Herein, the modified DRL mechanism is referred to as $DRL(\xi)$ mechanism.

Let mobile anchor move in a constant speed v. Let l_{basic} denote the length of a *basic segment* that mobile anchor moves during time period T. We have $l_{basic} = vT$. Firstly, we divide the monitoring region into several *basic segments* as shown in Fig. 11(a). Let the length and width of the given monitoring region be L and W, respectively, where $L = mvT$ and $W = 2nr$. This implies that there are m *basic segments* in each row. Moreover, as shown in Fig. 11(b), the *basic segment* l_{basic} can be further divided into two subsegments: the *tone subsegment* l_{tone} and *silence subsegment* $l_{silence}$, which denote the lengths traversed by mobile anchor in durations ξ and $T - \xi$, respectively. Let *starting tone point* (*STP*) and *starting silence point* (*SLP*) denote the start points of subsegments l_{tone} and $l_{silence}$, respectively, as shown in Fig. 11(b).

Since mobile anchor has similar behaviors in each *basic segment*, we concentrate our analysis on a *basic segment*. Fig. 12(a) depicts one *basic segment*. When the mobile anchor

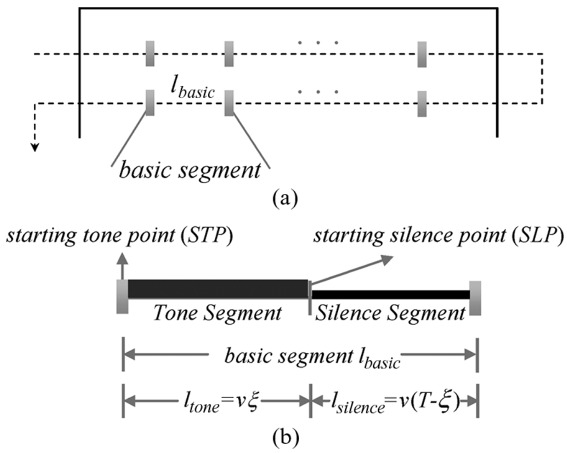

Fig. 11. The monitoring region can be divided into several *basic segments*.

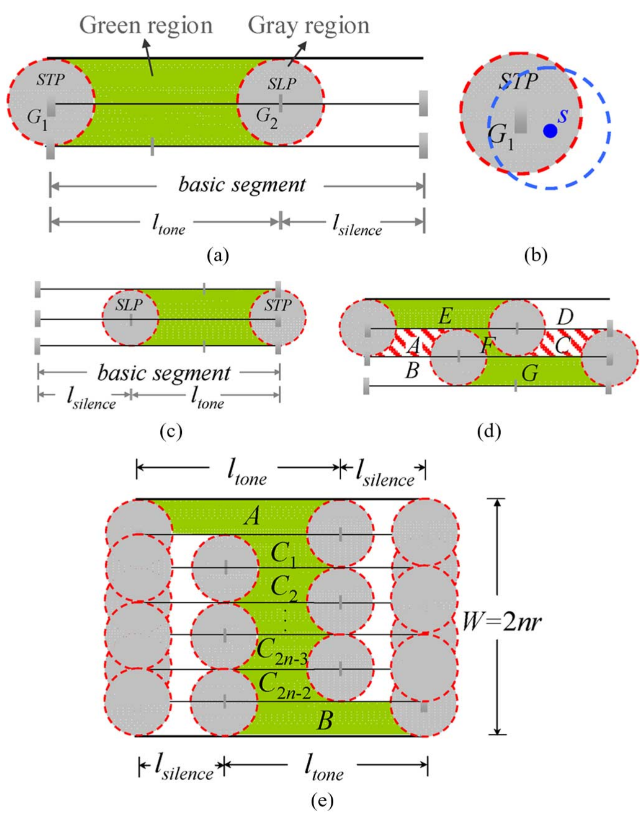

Fig. 12. Sensors located in the green regions can receive boundary tones while sensors located in the gray regions are s_{abg}^{enter} or s_{abg}^{leave}, respectively.

moves along this segment, the region swept by its communication range will form a pipe region which can be partitioned into gray, green and white regions. We notice that the tone signal broadcasted at the boundary of communication range of a sensor is very important for that sensor, since the sensor might enter or leave the tone range at that moment. Let *boundary tones* of a sensor, say s, denote the tone signals that are broadcasted at the boundary of communication range of sensor s. To apply the proposed mechanism, it is the basic requirement that the *entering boundary tone* and *leaving boundary tone* should be received by each sensor.

Let *ambiguous sensor* denote the sensor that misses *entering boundary tone* or *leaving boundary tone*. A sensor is said to be *Missing_Enter* (*Missing_Leave*) sensor, denoted by notation s_{abg}^{enter} (s_{abg}^{leave}) if it cannot receive *entering* or *leaving boundary tones*, respectively. As shown in Fig. 12(a), sensors located in the gray regions G_1 and G_2 are s_{abg}^{enter} and s_{abg}^{leave}, respectively. Fig. 12(b) gives an example to further observe the gray region. Let sensor s be arbitrary sensor located in G_1, as shown in Fig. 12(b). Because the *starting tone point* is within the communication range of sensor s, sensor s can not receive the *entering boundary tone*. Therefore, sensor s must be s_{abg}^{enter}. Similarly, sensors located in the gray region G_2 are s_{abg}^{leave}. Contrarily, the sensors located in green region can completely receive both *entering* and *leaving boundary tones* and thus can successfully distinguish their relative locations with their neighbors. In addition, the sensors located at white region (silence region) cannot receive any tone signals and thereby cannot successfully distinguish their relative locations with each of their neighbors. To calculate the success rate of distinguishing relative locations, we only need to measure the number of sensors in green and gray regions of a *basic segment*.

Since the mobile anchor applies snake-like movement, without loss the generality, we assume that the mobile anchor moves along right and left directions at odd and even rows, respectively. Fig. 12(a) and (c) depict the *basic segments* belonging to odd and even rows, respectively. Let N_{Green} denote the number of sensors in the green region of a *basic segment*. For a given WSN with network density d, (9) evaluates the value of N_{Green} of Fig. 12(a)

$$N_{Green} = d(2r \times l_{tone} - \pi r^2) = d(2rv\zeta - \pi r^2). \tag{9}$$

Similarly, in the even row, the mobile anchor moves along left direction and thus the green area is given as shown in Fig. 12(c). Equation (9) can be similarly applied to derive the value of N_{Green} of Fig. 12(c). Fig. 12(d) is obtained by combining Fig. 12(a) and (c). In Fig. 12(d), zone A is marked with red shadow regions which indicate that sensors in the zone cannot distinguish its relative location with all neighbors. This is because that all sensors in zone B are ambiguous sensors since they can receive neither *entering boundary tone* nor *leaving boundary tone*. As a result, all sensors in zone A cannot distinguish their relative locations with the neighbors located in zone B. Similarly, sensors located in zone C cannot distinguish their relative locations with the neighbors located in zone D. Let ϕ_i denote the area of zone i. The value of N_{Green} of Fig. 12(d) can be derived by (10) after ignoring zones A and C

$$\begin{aligned} N_{Green} &= d(\phi_E + \phi_G + \phi_F) = d(2\phi_E + \phi_F) \\ &= d\left[2\left(r \times l_{tone} - \frac{1}{2}\pi r^2\right)\right. \\ &\qquad \left. + r(l_{basic} - 2 \times l_{silence}) - \frac{1}{2}\pi r^2\right] \\ &= d\left(4rv\xi - rvT - \frac{3}{2}\pi r^2\right). \end{aligned} \tag{10}$$

According to (10), we can apply the concept to any column of the monitoring region. Let N_{Green}^{column} denote the number of sensors in the green region of any column of the monitoring region. As shown in Fig. 12(e), since $\phi_A = \phi_B$ and $\phi_{C_1} =$

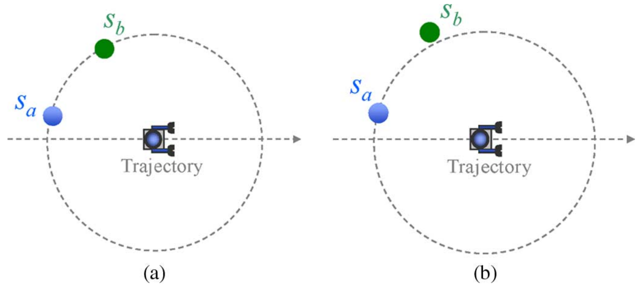

Fig. 13. Two situations that the relative locations cannot be correctly determined.

$\phi_{C_2} = \cdots = \phi_{C_{2n-2}}$, the value of N_{Green}^{column} of Fig. 12(e) can be calculated by (11)

$$\begin{aligned} N_{Green}^{column} &= d\left(\phi_A + \phi_B + \phi_{C_1} + \phi_{C_2} + \cdots + \phi_{C_{2n-2}}\right) \\ &= d\left[2\phi_A + (2n-2)\phi_{C_1}\right] \\ &= d\left\{2\left(r \times l_{tone} - \frac{1}{2}\pi r^2\right)\right. \\ &\qquad \left. + (2n-2)\left[r(l_{basic} - 2 \times l_{silence}) - \frac{1}{2}\pi r^2\right]\right\} \\ &= d\left[(4n-2)rv\xi - (2n-2)rvT - n\pi r^2\right]. \end{aligned} \tag{11}$$

Recall that $L = mvT$. That is to say, there are m columns in the monitoring region. Hence, the total number of sensors in the green regions, denoted by N_{Green}^{total}, of the monitoring region can be calculated by applying

$$N_{Green}^{total} = m \times N_{Green}^{column}. \tag{12}$$

Let P_{Green} denote the success rate of sensors that are not located in the green regions. Equation (13) derives the value of P_{Green}

$$P_{Green} = N_{Green}^{total}/LWd. \tag{13}$$

The following analyzes the number of sensors located in gray regions G_1 and G_2 as shown in Fig. 12(a). Recall that all sensors located in G_1 are s_{abg}^{enter} since they miss entering boundary tone. By applying the proposed *ETA* and *XTA Rules*, some sensors in G_1 might be able to distinguish their relative locations with all its neighbors. Nevertheless, there are two situations that the sensors applying the *ETA* and *XTA Rules* will obtain wrong relative location information. First, the pair of neighboring sensors leaves the tone-signal range at the same time, as shown in Fig. 13(a). In this situation, applying the *ETA* and *XTA Rules* cannot determine their relative location. Fig. 13(b) depicts the second situation. Applying *ETA Rule*, sensor s_b will believe that it is located at the left side of s_a, which is invalid. As a result, the relative location cannot be correctly determined. Next, we calculate the success probability of distinguishing relative locations in G_1 by analyzing the occurrence probabilities of these two situations.

We firstly discuss the occurrence probability of the first situation. Let (p,q) be the location of the *tone point*. Assume that the current location of mobile anchor is $(p+k,q), 0 \le k \le 2r$. Consider Fig. 14(a). Let the red and blue arcs denote the boundary of transmission range with the thickness α. Let notation ϕ_{arc}^k denote the area of shadow yellow arc which is the intersection region of G_1 and blue arc regions when mobile anchor is located at location $(p+k,q)$, as shown in Fig. 14(b). If ϕ_{arc}^k is populated by any pair of neighboring sensors, it represents that the two sensors will leave tone-signal range at the same time. To calculate the occurrence probability of this situation in G_1, we have to derive the value of ϕ_{arc}^k by varying the value of k.

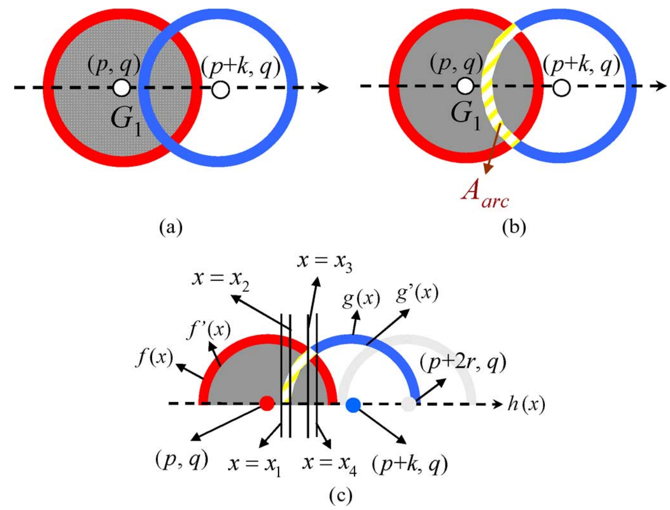

Fig. 14. The mobile anchor moves from $STP(p,q)$ to location $(p+2r,q)$.

As shown in Fig. 12(c), consider the trajectory that the mobile anchor starts moving from the $STP(p,q)$ to location $(p+2r,q)$ during time period $[t_1,t_2]$. The value of the current ϕ_{arc}^k can be derived by (14), where $f(x)$ and $f'(x)$ denote the outer-arc and inner-arc equations of red arc, respectively, and $g(x)$ and $g'(x)$ denote the outer-arc and inner-arc equations of blue arc, and $h(x) = q$

$$\begin{aligned} \phi_{arc}^k = 2 \times \Bigg\{ &\int_{x_3}^{x_4} [f(x) - g'(x)]\,dx + \int_{x_2}^{x_3} [g(x) - g'(x)]\,dx \\ &+ \int_{x_1}^{x_2} [g(x) - h(x)]\,dx \Bigg\}. \end{aligned} \tag{14}$$

Since the number of sensors located in the shadow yellow arc can be measured by the given network density d, the probability of any sensor located in the yellow arc $p_{arc}^{single}(k)$ can hence be derived as follows:

$$p_{arc}^{single}(k) = \left(\phi_{arc}^k \times d\right)/(\pi r^2 \times d) = \phi_{arc}^k/\pi r^2. \tag{15}$$

The probability of another sensor also located in the yellow arc $p_{arc}^{pair}(k)$ can further be derived as

$$p_{arc}^{pair}(k) = p_{arc}^{single}(k) \times \left(d \times \phi_{arc}^k - 1\right)/(d \times \pi r^2 - 1). \tag{16}$$

On the other hand, the following discusses the occurrence probability of the second situation as shown in Fig. 13(b). As shown in Fig. 15, let L_a denote the line passing through $loc(s_a)$ but parallelizing to y-axis. Let point b be the intersection point of L_a' and communication circle of the mobile anchor, and the distance between $loc(s_a)$ and $loc(b)$ is r. We can obtain the line L_a' by rotating the L_a until it reaches point b. Let θ denote the

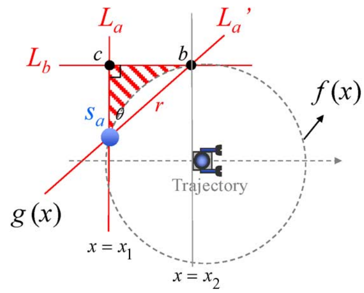

Fig. 15. If any sensor located in the shadow red region, it must leave the tone-signal range earlier than s_a.

angle of L_a and L'_a. Let L_b denote the line passing through $loc(b)$ but perpendicular to L_a, and point c is the intersection point of L_a and L_b. Any sensor located in the red region must leave the tone-signal range earlier than s_a, and thus the second situation occurs.

The area size of shadow red region ϕ_{red}, as shown in Fig. 15, is firstly calculated because it is helpful for deriving the occurrence probability of the second situation. Let $f(x)$ and $g(x)$ denote the equations of the communication circle of mobile anchor and the straight line L'_a, respectively. It is obvious that lines L_a, L'_a, and L_b can form a right triangular region. Let $\phi_{triangular}$ and ϕ_{green} denote the areas of the right triangular region and the green region shown in Fig. 15. Let $dis(i,j)$ denote the distance between locations i and j. The value of ϕ_{red} can be derived by

$$\begin{aligned}\phi_{red} &= \phi_{triangular} - \phi_{green}\\ &= \frac{1}{2}\left[dis\left(loc(c), loc(s_a)\right) \times dis\left(loc(c), loc(b)\right)\right]\\ &\quad - \int_{x_1}^{x_2} \left[f(x) - g(x)\right] dx. \end{aligned} \tag{17}$$

Let p_{red} denote the probability that any sensor is located at the shadow red region. Equation (18) calculates the value of p_{red}

$$p_{red} = (d \times \phi_{red})/(d \times \pi r^2) = \phi_{red}/\pi r^2. \tag{18}$$

The number of G_1 is $m(2n-1)$ in the monitoring region. Let P_{G1} denote the success probability of sensors that are located at G_1. Equation (19) derives the value of P_{G1}

$$P_{G1} = m(2n-1)\left(1 - \sum_{k=0}^{2r} p_{arc}^{pair}(k) - d\pi r^2 \times p_{red}\right). \tag{19}$$

Similarly, we can also evaluate the value of P_{G2} which is the success probability in gray region G_2 as shown in Fig. 12(a).

Equation (20) considers the green and gray regions together and derives the success probability $P_{horizontal}$ of $DRL(\xi)$ when the mobile anchor moves along the horizontal direction

$$P_{horizontal} = P_{Green} + P_{G1} + P_{G2}. \tag{20}$$

Similarly, we can also derive the success probability $P_{vertical}$ of $DRL(\xi)$ when the mobile anchor moves along the vertical direction. Hence, the overall success probability $P_{success}$ of the proposed $DRL(\xi)$ for distinguishing the relative locations of any pair of sensors can be derived as

$$P_{success} = P_{horizontal} \times P_{vertical}. \tag{21}$$

The following gives the summarized observation from the above analysis. The value of N_{Green}^{total} is increased with the value of ξ as shown in (12) while the value of P_{Green} is increased with the value of N_{Green}^{total} as shown in (13). As a result, the values of $P_{horizontal}$ and $P_{success}$ as shown in (20) and (21) will be increased with the value of ξ. We can accordingly conclude that the performance of $DRL(\xi)$ is increased with the value of ξ.

TABLE II
SIMULATION PARAMETERS

Network size	: 300m × 300m
Transmission range	: 30m ~ 70m
Network density	: 0.006 ~ 0.02 nodes/m^2
Cycle length T	: 10 ~ 100 sec
The value of ξ	: 10 ~ 100 sec
The value of β	: 0, 25, 50 %
Tone scheduling	: continuous, periodic
Tone transmission cost	: 0.030 J/s
Mobility cost	: 8.267 J/m

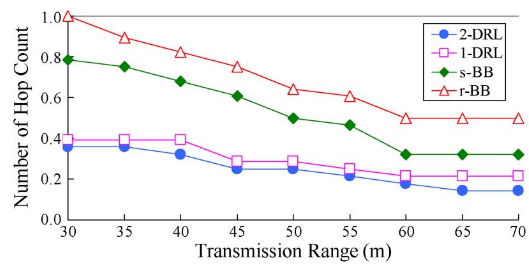

Fig. 16. The comparison of four mechanisms in terms of routing length.

VI. SIMULATION STUDY

This section compares the performances of the proposed *Two-Phase DRL* and *Single-Phase DRL* mechanisms against the traditional bounding-box mechanisms *r-BB* and *s-BB* [4]. The only difference between *r-BB* and *s-BB* is the way of their movements. More specifically, in the *r-BB* mechanism, the mobile anchor randomly moves and broadcasts its location information to the sensors for localization purpose. Different from the *r-BB*, the *s-BB* moves the anchor following a snake-like trajectory. The parameters used in our simulation are listed in Table II. Each simulation result is obtained from the average of 100 independent runs. The following depicts the results of our performance study.

Fig. 16 verifies the impact of relative location information on routing performance. The location aware routing protocol [5] is applied to construct a route between two sensors that are at right 300 m distance away. Fig. 16 gives the general results of routing length comparisons. The value of routing length is normalized between 0 and 1. In general, the numbers of hop counts of the compared four mechanisms are decreased with the transmission range. This is because that the location-aware routing mechanism always selects the node that is closest to the destination as its next-hop relay node. The proposed *Two-Phase DRL* and

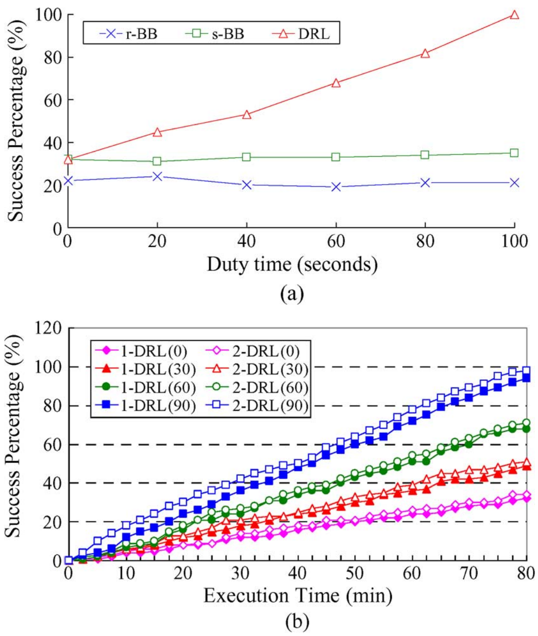

Fig. 17. The ipacts of duty time ξ on the success percentage of distinguishing relative locations.

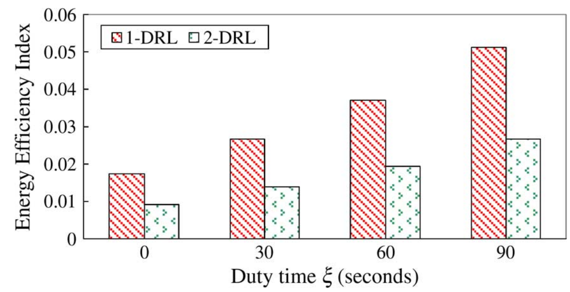

Fig. 18. The comparison of the proposed mechanisms in terms of EEI.

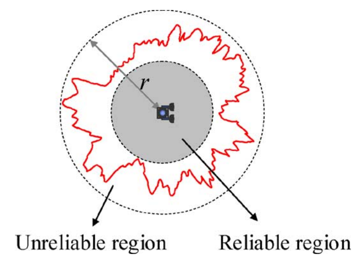

Fig. 19. The radio propagation pattern.

Single-Phase DRL mechanisms outperform the compared $s-BB$ and $r-BB$ mechanisms in terms of routing length. Since the *Two-Phase DRL* and *Single-Phase DRL* mechanisms provide more accurate relative location information than the compared two mechanisms, they have better results. The average routing length by applying *Two-Phase DRL* and *Single-Phase DRL* mechanisms are similar since they help most of sensors identify the relative locations with each of their neighbors. The $s-BB$ and $r-BB$ lead to a poor situation where a number of sensors cannot identify the relative locations with their neighbors due to the overlapped bounding-box.

Fig. 17(a) and (b) investigate the success percentage of distinguishing relative locations of any two neighboring sensors. As shown in Fig. 17(a), three mechanisms are compared by varying the duty time ξ. The success percentages of $r-BB$ and $s-BB$ are not impacted by parameters ξ and always keep a constant value. On the contrary, the success percentage of the proposed DRL mechanism increases with ξ. Given a fix value of cycle length $T = 100$, the number of sensors receiving tone signals is increased with ξ. The major reason is that each of these sensors and its neighbors can distinguish their relative locations based on the received tone signals. In particular, when the ξ value is equal to zero, it means that the mobile anchor did not broadcast any tone signal and hence the $s-BB$ and the proposed DRL mechanisms have the same success percentage.

Similarly, as shown in Fig. 17(b), given a fix value of cycle length $T = 90$, the value of duty time ξ is varied by 0, 30, 60, and 90. In particular, the mobile anchor always broadcasts tone signal in case that the value of ξ is 90 while the mobile anchor always keep silence without broadcasting any tone signal if the value of ξ is 0. As shown in Fig. 17(b), the success percentages of both the proposed *Two-Phase DRL* and *Single-Phase DRL* mechanisms are increased with the value of ξ. This also verifies that the tone signals can improve the success percentage for neighboring sensor to distinguish their relative locations. Note that the proposed *Two-Phase DRL* and *Single-Phase DRL* mechanisms have similar success percentages. Recall that the *Single-Phase DRL* mechanism can save more energy consumption and time than *Two-Phase DRL* mechanism. Compared with the *Two-Phase DRL* mechanism, the *Single-Phase DRL* mechanism is more cost-effective since it achieves a similar success percentage but save more energy and time.

The following introduces the *Energy Efficiency Index* (*EEI*) to estimate the contribution of each unit of energy consumption in terms of increased success percentage. The EEI is formulated as

$$EEI = \frac{\text{Success Percentage}}{\text{Total Energy Consumption for Mobile Anchor}}.$$

Herein, we notice that the mechanism which results in the largest value of EEI would be the most cost-effective approach. As shown in Fig. 18, the EEI values obtained by applying the *Single-Phase DRL* mechanism are larger than those obtained by applying the *Two-Phase DRL* mechanism in all cases. In particular, when $\xi = 0$, the *Two-Phase DRL* mechanism has the smallest value of EEI and thus has the least contribution in terms of success percentage. In this case, the mobile anchor moves without broadcasting any tone. Thus, a lot of energy is consumed for movement but contributes nothing to the success percentage. On the contrary, when the mobile anchor applies the *Single-Phase DRL* mechanism and broadcasts the tone signal all the time ($\xi = 90$), the value of EEI is largest, which indicates that it is the most cost-effective. This is because that the *Single-Phase DRL* mechanism has a shorter path length than *Two-Phase DRL* mechanism but can likely help all neighboring sensors distinguish their relative locations.

The following discusses the impact of radio propagation pattern on the DRL performance. As shown in Fig. 19, let r denote the transmission range of the mobile anchor. Let the gray and

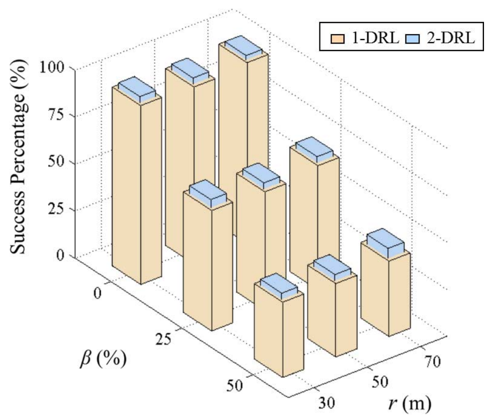

Fig. 20. The impacts of transmission range r and the value of β on success percentage of distinguishing relative locations.

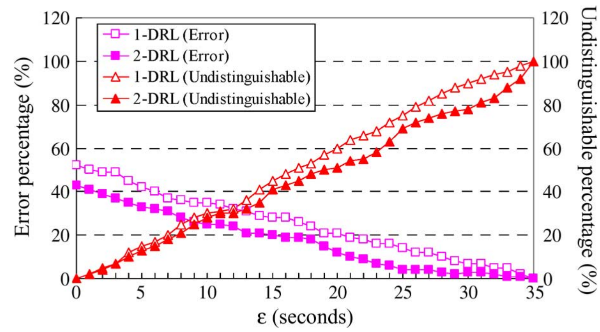

Fig. 21. The impacts of ignoring time ε on the error and undistinguishable percentages for distinguishing relative locations of any two neighboring sensors.

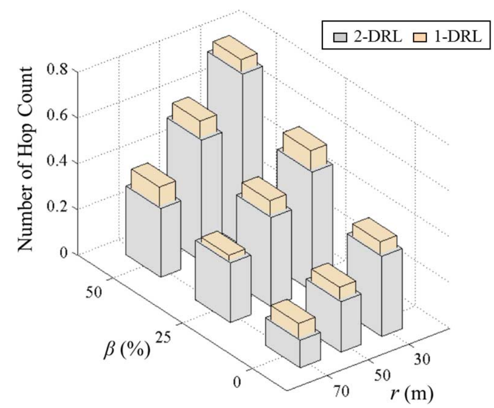

Fig. 22. The impacts of transmission range r and the value of β on routing performance.

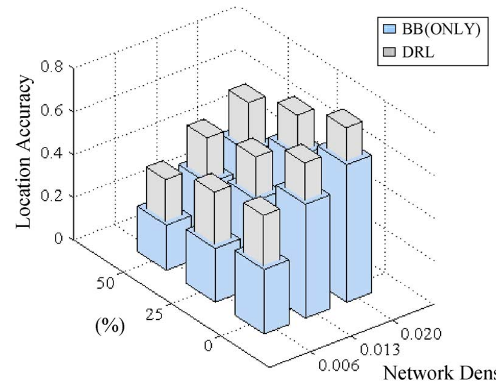

Fig. 23. The impacts of network density and the value of β on location accuracy.

white regions represent *reliable* and *unreliable regions*, respectively. A sensor located in the reliable region can receive the tone signal from the mobile anchor. On the contrary, the sensor located in the unreliable region might not receive the tone signal.

Fig. 20 investigates the success percentage of the proposed mechanisms. Let β denote ratio of unreliable region to the whole transmission range. Note that a large value of β implies significant background noise. The *Two-Phase DRL* and *Single-Phase DRL* mechanisms are compared by varying the transmission range r and the value of β. As shown in Fig. 20 the success percentages of two mechanisms are significantly impacted by β. The major reason is that two neighboring sensors might not correctly apply the order of entering or leaving tone signals to determine their relative locations. For example, consider two neighboring pair of sensors a and b where location of a is at the left side of location b. In case that the transmission range is a perfect circle, sensor a will receive the tone signal prior to sensor b in most cases. However, if the transmission is unreliable, sensor b might receive the tone single earlier than sensor a in most cases, which causes an invalid decision to their relative locations.

Let the notation ε denote the length of *ignoring time* for each sensor. That is, each sensor will consider that it receives the first tone signal after it actually receives tone signal for a time period of ε. This extension of the proposed DRL mechanisms should be helpful to cope with the problem raised by unreliable region of transmission range.

Fig. 21 investigates the error and undistinguishable percentages for distinguishing relative locations of any two neighboring sensors. The *Two-Phase DRL* and *Single-Phase DRL* mechanisms are compared by varying the value of ε. As shown in Fig. 21, the error percentages of two mechanisms are decreased with ε. It is because that the larger value of ε leads to a smaller impact on background noise. On the contrary, the undistinguishable percentages of two mechanisms are increased with ε. The major reason is that the larger value of ε results in a large number of tone signals ignored by the sensors.

Fig. 22 further investigates the impact of β on the average routing length. The location aware routing protocol [5] is also applied to construct a routing between two sensors that are right 300 m distance away. The *Two-Phase DRL* and *Single-Phase DRL* mechanisms are compared by varying the values of r and β. As shown in Fig. 22, the average routing lengths are decreased with r. This is because that the location-aware routing mechanism always selects the node that is closest to the destination as its next-hop relay node. The average distance of each hop is increased with r. Hence, a larger value of r results in a smaller routing length. In addition, a larger β value represents a bigger size of unreliable region, which is the major reason for causing an invalid decision of relative location. Consequently, the routing length is increased with the value of β.

Fig. 23 investigates the improvement of location accuracy by applying the proposed DRL. The value of β is varied from 0 to 50 and the network density is set by 0.006, 0.013 or 0.02. The BB mechanism only applies bounding box mechanism as the localization scheme while the $DRL+BB$ applies both BB and the proposed DRL mechanisms. The location accuracy is measured by the average size of bounding box of each sensor and its value is normalized between 0 and 1. As a result, the location accuracy is impacted by network density. Herein, we notice that the neighboring sensors can help with each other to reduce the sizes of their bounding-box. Since the number of neighboring sensors is increased with the network density, the location accuracy is increased when the network density is high. In addition, a larger value of β creates a higher error rate for distinguishing the relative locations of each neighboring pair. As a result, the location accuracy is decreased with the value of β. In general, the $DRL+BB$ mechanism outperforms the BB mechanism in terms of location accuracy.

VII. Conclusions

Distinguishing relative location of neighboring sensors can help find a valid forwarder for wireless sensor networks, especially in the environment where each sensor has an inaccurate location-information like bounding-box. This paper proposes *Two-Phase DRL* and *Single-Phase DRL* mechanisms which adopt tone signals to help each sensor identify its relative locations with any of its neighbor. Firstly, a *General Rule* is proposed for the general case that the order of entering or leaving tone-signal range can be distinguished. However, for some special cases, the *Table* and *Location Ambiguous Problems* occur. To cope with the problems, the *Table Ambiguous Rules* and *Location Ambiguous Rule* are further proposed. The proposed four rules can be implemented in each sensor for identifying its relative location with its neighbors. In addition, two path planning mechanisms are proposed to guarantee that all sensors can receive the tone signals with low energy consumption of the mobile anchor. Simulation results depict that the proposed DRL mechanisms not only improve the average location accuracy of sensors but also improve the performance of routing.

References

[1] J. P. Sheu, W. K. Hu, and J. C. Lin, "Distributed localization scheme for mobile sensor networks," *IEEE Trans. Mobile Comput.*, vol. 9, no. 4, pp. 516–526, April 2010.

[2] B. Xiao, H. Chen, and S. Zhou, "Distributed localization using a moving beacon in wireless sensor networks," *IEEE Trans. Paral. Distr. Syst.*, vol. 19, no. 5, pp. 587–600, May 2008.

[3] S. Zhang, J. Cao, L. Chen, and D. Chen, "Locating nodes in mobile sensor networks more accurately and faster," presented at the IEEE Communications Society Conf. on Sensor and Ad Hoc Communications and Networks (SECON'05), Sep. 2005.

[4] A. Galstyan, B. Krishnamachari, K. Lerman, and S. Pattem, "Distributed online localization in sensor networks using a moving target," presented at the IEEE/ACM Int. Symp. on Information Processing in Sensor Networks (IPSN'04), Apr. 2004.

[5] H. Zhang and H. Shen, "Energy-efficient beaconless geographic routing in wireless sensor networks," *IEEE Trans. Paral. Distr. Syst.*, vol. 21, no. 6, pp. 881–896, Jun. 2010.

[6] H. Frey and I. Stojmenovic, "On delivery guarantees and worst-case forwarding bounds of elementary face routing components in ad hoc and sensor networks," *IEEE Trans. Comput.*, vol. 59, no. 9, pp. 1224–1238, Sep. 2010.

[7] Y. Sun, Q. Jiang, and M. Singhal, "An edge-constrained localized Delaunay graph for geographic routing in mobile ad hoc and sensor networks," *IEEE Trans. Mobile Comput.*, vol. 9, no. 4, pp. 479–490, Apr. 2010.

[8] W. J. Liu and K. T. Feng, "Greedy routing with anti-void traversal for wireless sensor networks," *IEEE Trans. Mobile Comput.*, vol. 8, no. 7, pp. 910–922, Jul. 2009.

Chih-Yung Chang received the Ph.D. degree in computer science and information engineering from National Central University, Taiwan, in 1995.

He joined the faculty of the Department of Computer and Information Science, Aletheia University, Taiwan, as an Assistant Professor in 1997. He was the Chair of the Department of Computer and Information Science, Aletheia University, from August 2000 to July 2002. Since August 2002, he has been an Associate Professor with the Department of CSIE, Tamkang University. He is currently a Full Professor with the Department of CSIE at Tamkang University, Taiwan. His current research interests include wireless sensor networks, Bluetooth radio networks, Ad Hoc wireless networks, and WiMAX broadband technologies.

Dr. Chang is a member of the IEEE Computer Society, Communication Society and IEICE society. He served as an Associate Guest Editor of *IET Communications* (2011), *Telecommunication Systems* (TS, 2010), *Journal of Information Science and Engineering* (JISE, 2008), *Journal of Internet Technology* (JIT, 2004 & 2008), *Journal of Mobile Multimedia* (JMM, 2005), and a member of Editorial Board of *Tamsui Oxford Journal of Mathematical Sciences* (2001–2008) and *Journal of Information Technology and Applications* (JITA, 2008). He was an Area Chair of IEEE AINA'2005, Vice Chair of IEEE WisCom'2005 and EUC'2005, Track Chair (Learning Technology in Education Track) of IEEE ITRE'2005, Program Co-Chair of WASN'2007, MNSAT'2005 and UbiLearn'2006, Workshop Co-Chair of ICS'2008, INA'2005, MSEAT'2003, MSEAT'2004, and Publication Chair of MSEAT'2005 and SCORM'2006.

Chih-Yu Lin received the B.S. degree in computer science and information engineering from Aletheia University, Taiwan, in 2007, and the M.S. degree in computer science and information engineering from Tamkang University, Taiwan, in 2009, where he is working toward the Ph.D. degree. His research domains include wireless sensor networks, Ad-Hoc wireless networks, mobile/wireless computing, and WiMAX.

Mr. Lin won numerous scholarships in Taiwan and participated in many wireless sensor networking projects.

Chao-Tsun Chang was born in Taipei, Taiwan. He received the Ph.D. degree in computer science and information engineering from National Central University, Taiwan, in 2006.

He joined the faculty of the Department of Department of Information Management, Hsiuping University of Science and Technology, Taiwan, as an Assistant Professor in 2006. In the past 10 years, he has directed 11 researching projects including three national NSC projects and eight information system developments. His current research interests include wireless sensor networks, Bluetooth radio networks, Ad Hoc wireless networks, and mobile computing.

Dr. Chang is a member of the IEEE Computer Society and Communication Society.